BNL-95068-2011-CP

Growth of detector-grade CZT by Traveling Heater Method (THM): An advancement

U.N. Roy, S. Weiler, J. Stein, M. Groza, A. Burger, A.E. Bolotnikov, G.S. Camarda, A. Hossain, G. Yang, and R.B. James

Presented at the 2011 MRS Spring Meeting and Exhibit Conference
San Francisco, California
April 25-29, 2011

April 2011

Nonproliferation and National Security Department

Brookhaven National Laboratory

U.S. Department of Energy
National Nuclear Security Administration, Office of Science

DISCLAIMER

Growth of detector-grade CZT by Traveling Heater Method (THM): An advancement

U. N. Roy[1], S. Weiler[1], J. Stein[1], M. Groza[2], A. Burger[2], A. E. Bolotnikov[3], G. S. Camarda[3], A. Hossain[3], G. Yang[3] and R. B. James[3]

[1]FLIR Radiation Inc., 100 Midland Road, Oak Ridge, TN 37830
[2]Department of Physics, 1000, 17th Avenue North, Fisk University, Nashville, TN 37208
[3]Brookhaven National Laboratory, Upton, NY 11793

ABSTRACT

In this present work we report the growth of $Cd_{0.9}Zn_{0.1}Te$ doped with In by a modified THM technique. It has been demonstrated that by controlling the microscopically flat growth interface, the size distribution and concentration can be drastically reduced in the as-grown ingots. This results in as-grown detector-grade CZT by the THM technique. The three-dimensional size distribution and concentrations of Te inclusions/precipitations were studied. The size distributions of the Te precipitations/inclusions were observed to be below the 10-μm range with the total concentration less than 10^5 cm^{-3}. The relatively low value of Te inclusions/precipitations results in excellent charge transport properties of our as-grown samples. The $(\mu\tau)_e$ values for different as-grown samples varied between 6-20 $x10^{-3}$ cm^2/V. The as-grown samples also showed fairly good detector response with resolution of ~1.5%, 2.7% and about 3.8% at 662 keV for quasi-hemispherical geometry for detector volumes of 0.18 cm^3, 1 cm^3 and 4.2 cm^3, respectively.

INTRODUCTION

In spite of ongoing active research to develop novel room-temperature detector materials, CdZnTe (CZT) has continued to be the most promising semiconductor material for room-temperature nuclear detector applications for almost two decades. Presently there is an increasing demand for larger volume, especially larger thickness (>10 mm) CZT detectors for homeland security applications for fast and unambiguous nuclide identification. Thicker detectors also provide sufficient stopping power for higher energy gammas and better standoff detection. Although the Travelling Heater Method (THM) technique is well established for the growth of large-volume single crystalline CZT crystals, the main bottleneck until today has been the requirement for post-growth annealing for detector applications [1, 2]. The THM technique offers many advantages over melt-growth techniques. The main advantage is the fairly uniform Zn concentration along the growth direction [3, 4]. The uniform Zn concentration is essential for good charge transport especially for thick detectors in addition to better yield. As it is well known that THM is a lower temperature growth process compared to Bridgman (i.e., much below that the melting point of CZT), advantages of lower growth temperature are less or no chance of explosion of the growth ampoule, less contamination from the crucible, and less defect density. Schoenholz et al. [5] reported lower etch pit density for THM-grown CdTe compared to Bridgman-grown CdTe. They also demonstrated that the defect density reduces drastically in the grown crystal compared to the seed. Recently Gang et al. [6] demonstrated that Te acts as a

gettering agent for impurities, this also is an added advantage of self-purification of the grown ingots from the Te-rich solvent by the THM technique. Thus, crystals with less thermal stress, less defects and higher purity with composition uniformity can be grown by a THM technique. The THM technique however has the main disadvantage of having Te-rich CZT and CZT interface. This interface is the cause for added Te inclusions in the grown ingots other than the formation of Te precipitations due to retrograde solubility. In order to minimize the formation of Te inclusions during growth from the interface, a microscopically flat and clean interface is essential to achieve as-grown detector-grade material. It is well known now that the Te inclusions/precipitations have detrimental effect on the device performance [7,8]. The main purpose for post-growth annealing is the removal of relatively large (> 5-10-micron diameter) Te inclusions formed during growth. Minimization of Te inclusions originating at the interface during THM growth results in as-grown detector-grade material with good charge transport properties. The elimination of the post-growth annealing process will reduce production costs and improve the availability of large-size detectors. In this paper we will discuss the volumetric size distribution and concentration of Te precipitations/inclusions of as-grown CZT crystals and the minimization of Te inclusions by controlling the growth interface. Experimental data on charge transport properties, internal electric field estimation and detector performance of as-grown CZT samples will be presented and discussed.

EXPERIMENT

All the crystals were grown from as-received 6N purity CdZnTe from 5N Plus Inc. with the nominal concentration of 10% Zn. 6N purity Te from Alfa Aesar was used for the solvent, and 6N purity In was used as the dopant. The crystals were grown by the THM technique from a Te-rich solvent in conically tipped quartz ampoules. Prior to loading, the inner walls of the ampoules were coated with graphite by cracking high-purity acetone. The details of the growth procedure are discussed elsewhere [9].

The growth interfaces were investigated by cutting the wafers along the growth direction near the interface. The microscopic investigation of the interfaces was carried out on mirror-finished polished samples using a high magnification optical microscope (Zeiss Axio Imager M1m) after final polishing with a 0.05-μm alumina suspension. For IR transmission imaging of the full 52-mm diameter wafers, slabs were cut perpendicular to the growth direction and polished to mirror finish surface on both sides. An automated IR transmission microscopy system was used for mapping the Te inclusions/precipitates. The system comprises a large field-of-view microscope objective, a 3.5 x3.5 μm^2 pixel digital CCD camera that produces 2208x3000 pixel images, and a computer-controlled XYZ translation stage. Stacks of images were acquired, each focused at different depths in the wafers. The resolution of the IR imaging system is sufficient to quantify the Te inclusions/precipitates down to ~1 μm. We employed an iterative algorithm to identify the inclusions and evaluate their sizes. The experimental procedure is described in greater detail elsewhere [10].

Samples of different sizes were cut and polished from the as-grown ingots for charge transport measurements and detector fabrications. For charge transport measurements, planar gold electrodes were used by sputtering technique. A collimated ^{241}Am alpha source was used for the $(\mu\tau)_e$ measurements. The $(\mu\tau)_e$ values were estimated by plotting the charge collection efficiency versus applied voltage and then fitting to the Hecht equation. Different devices were fabricated with volumes ranging from ~0.2 cm^3 to over 4 cm^3 from the as-grown ingots. Most of the

devices were tested with a quasi-hemispherical geometry; the geometry consists of a pixelated anode and five-side cathode. All the contacts were produced from sputtered gold.

RESULTS AND DISCUSSION

The ingots were easily removed from the quartz ampoules without any sticking problem, mainly due to the graphite coating on the inner wall of the crucibles. A thin coating of Te was observed around the grown ingots. We are routinely growing 52-mm diameter ingots by THM technique, and most of the results presented here will be from 52-mm diameter ingots unless otherwise mentioned. As discussed earlier, there are two obvious sources for formation of Te inclusions/precipitations. One is common for both THM- and melt-growth techniques, which is the retrograde solubility. The size and concentration of the Te precipitations due to retrograde solubility are supposed to be less in THM-grown ingots compared to melt-grown ingots due to the lower temperature growth. The second reason for forming Te inclusions in THM-grown crystals is the trapping of Te-rich CZT at the growth interface. The trapping can be reduced or minimized by controlling the growth interface to become more microscopically flat, which is the key factor for achieving as-grown detector grade CZT. In addition to that, the macroscopic shape of the interface plays an important role in the grain growth. Flat/convex interface results in growth of single crystalline/large grain crystals. We are continuously trying to improve the growth interface in order to achieve a microscopically and macroscopically flat interface to minimize Te inclusions due to trapping and to increase the grain size. Figure 1 shows a typical as-grown ingot cut along the growth direction. The shiny portion near the top of the ingot is the Te-rich CZT solvent portion, and the interface between the Te-rich CZT and grown CZT is reasonably flat as shown in Fig. 1.

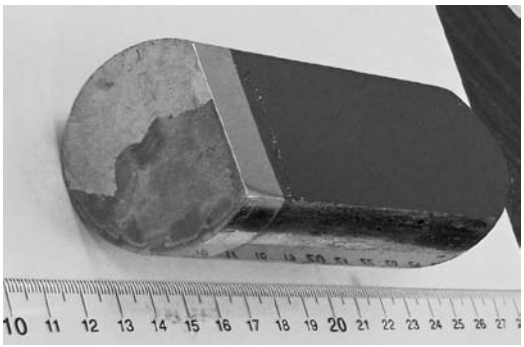

Fig. 1. 52-mm diameter CZT ingot by THM

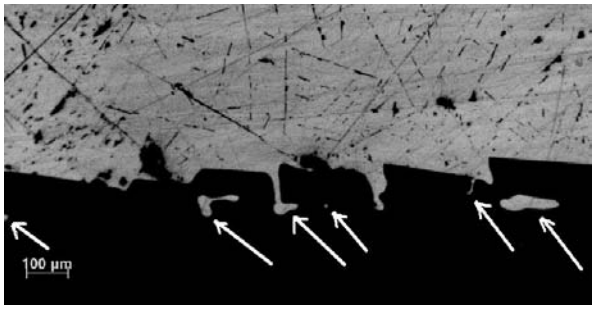

Fig. 2. Morphology of the growth interface

Figure 2 represents an optical micrograph taken in a reflecting mode; the irregular shape of the interface depicting the trapping of Te-rich CZT in the as-grown ingot is clear. The lower dark portion is the grown CZT, and the bright portion is the Te-rich CZT solvent. The trapping of Te-rich CZT at the interface is evident from Fig. 2, as shown by the arrows. These regions lead to Te-rich inclusions in the as-grown part of the ingot. In order to reduce the trapped Te-rich volumes, it is essential to achieve a microscopically flat interface resulting in as-grown detector grade CZT that is relatively free of Te inclusions.

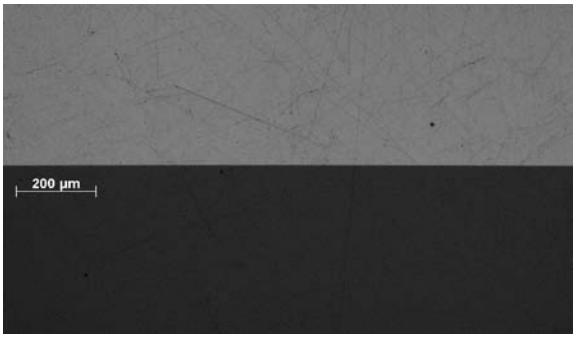

Fig. 3. Smooth growth interface

After optimization of our growth process, a microscopically flat interface could be achieved. Figure 3 is the typical representation of the microscopically flat interface and illustrates minimization of the trapped Te-rich CZT solution in the grown ingot. As shown in Fig. 2, the shapes of the trapped Te inclusions are highly irregular in nature. The trapped Te inclusions at the growth interface severely affect the yield and the device performance. Figure 4a shows the

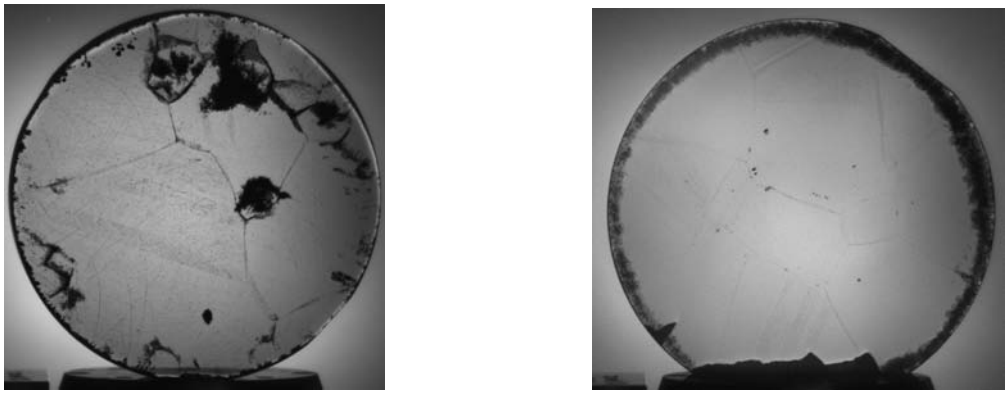

(a) **(b)**

Fig. 4. IR transmission image of a 52-mm diameter CZT. a) Example of trapped Te inclusions at the interface during growth; b) fairly clean wafer resulting from a microscopically clean melt-solid interface.

IR transmission image of a 52-mm diameter full wafer grown with an irregular growth interface. The black portions are the trapped Te-rich CZT solvent inclusions severely affect the detector yield. It demonstrates the importance of controlling the interface during growth. Figure 4b shows the relatively clean as-grown CZT wafer by THM technique from a microscopically flat growth interface after optimization of the growth parameters. It is to be noted that in most of the ingots, Te inclusions were found to be more concentrated near the periphery of the ingots as shown in Figs. 4a and 4b.

The size distribution and concentration of Te inclusions/precipitations are vital parameters for device-grade CZT materials. Presence of these defects, especially with sizes of 3 µm and larger are known to severely degrade the device performance, especially for long-drift-length (thicker detector) devices. Higher concentrations and larger sizes of the Te inclusions/precipitations in the CZT material restrict the use of thicker detectors as gamma-ray spectrometers. In order to evaluate our as-grown CZT crystals, we have investigated the size distribution and

concentrations of Te inclusions/precipitations present in the bulk of the crystals. Figure 5a shows a typical 3D volumetric distribution of Te inclusions/precipitations over the volume of 1x1.5x3 mm^3 for CZT grown using our THM method. The total concentration of the Te inclusions/precipitations over the scanned volume was estimated to be $1.3x10^5$ cm^{-3} and is comparable to the recently reported value for commercially available CZT samples [11]. The size distribution of the Te inclusions/precipitations over the same volume is shown in Fig. 5b. It is to be noted that the main

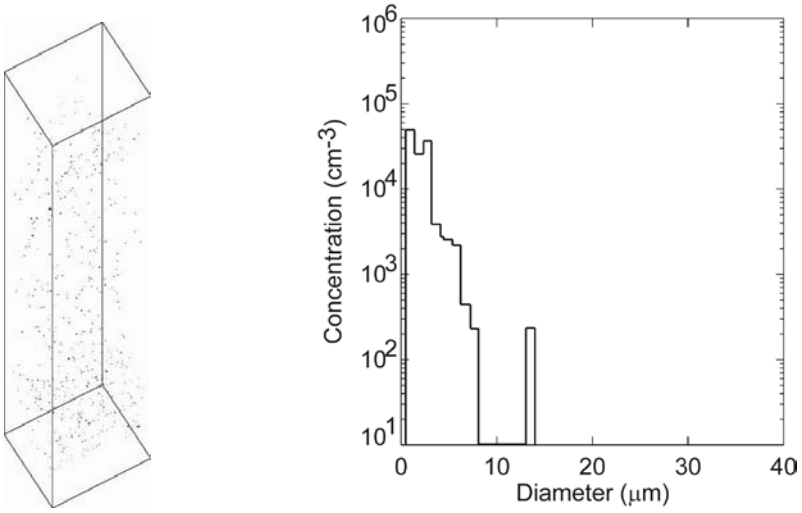

(a) **(b)**

Fig. 5. a) 3D distribution of Te inclusions/precipitates of the as-grown CZT sample within a 1x1.5x3 mm^3 volume; b) the size distribution over the same volume.

histogram extends below 10 μm, and was consistent at different positions of the wafers and also for different ingots, while the distribution was recently reported to be extend from 15-25 μm for many commercially available CZT samples [11]. It is also evident that most of the concentrations are around or below 3 μm as shown in Fig. 5b. The concentrations of Te precipitations/inclusions with a diameter of ~4 μm or larger was found to fall in the region of 6-8 $x10^3$ cm^{-3}. Bolotnikov et al. [12] found such small inclusions (size ~3 μm) degrade the device's performance only when their concentrations are above 10^6-10^7 cm^{-3}, while uniformly distributed inclusions below 1-μm size do not adversely affect performance. As shown in Fig. 5b, discrete occurrences of larger diameter Te precipitations /inclusions were also observed. In some places of the wafers even larger diameter up to 30-μm size inclusions were detected with a concentration of slightly higher than 100 cm^{-3}; these might be formed due to trapping of Te-rich solvent at the interface during growth. The simulation study however shows that for 15-mm thick detector, the resolution should be less than 2% at 662 keV for concentration of 10^3 cm^{-3} for 20-μm diameter size Te inclusions [12]. Thus, the size distribution and concentration of Te inclusions/precipitates in our as-grown CZT crystals by THM meet all the simulated requirements for fabricating 15-mm-thick detectors with good resolution.

Low temperature photoluminescence (PL) is a powerful tool to evaluate the quality of the material. Figure 6 shows the typical PL spectrum at 5 K for as-grown CZT by the THM technique. The sample was etched in 2% bromine-methanol solution prior to the measurement. The spectrum consists of three main regions; they are: i) near band edge region, ii) donor-acceptor region, and iii) defect band, generally known as the A-center. The spectrum consists of

a dominant donor-bound exciton (D^0, X) peak centered at 1.653 eV; the ground state free exciton peak (X_1) and the upper polariton band (X_{up}) are visible as shown in Fig. 6b. The dominant (D^0, X) peak and the observed free excitonic peak are the reflection of high-quality detector-grade material [13,14]. The sharpness of the (D^0, X) peak also is an indicator of the quality of the material [13]. The FWHM of the (D^0, X) peak after Lorentzian fitting was found to be 2.2 meV and agrees well with the reported value of ~ 3 meV [14]. The acceptor-bound exciton (A^0, X) was observed at the peak energy of 1.64 eV. The peak centered at an energy 1.618 eV was assigned as the LO phonon replica of (A^0, X), which we designate as (A^0, X-1LO). The donor acceptor pair (DAP) transition was observed at 1.605 eV as shown in Fig. 6c. The LO phonon replicas of DAP are also visibly seen in Fig. 6c.

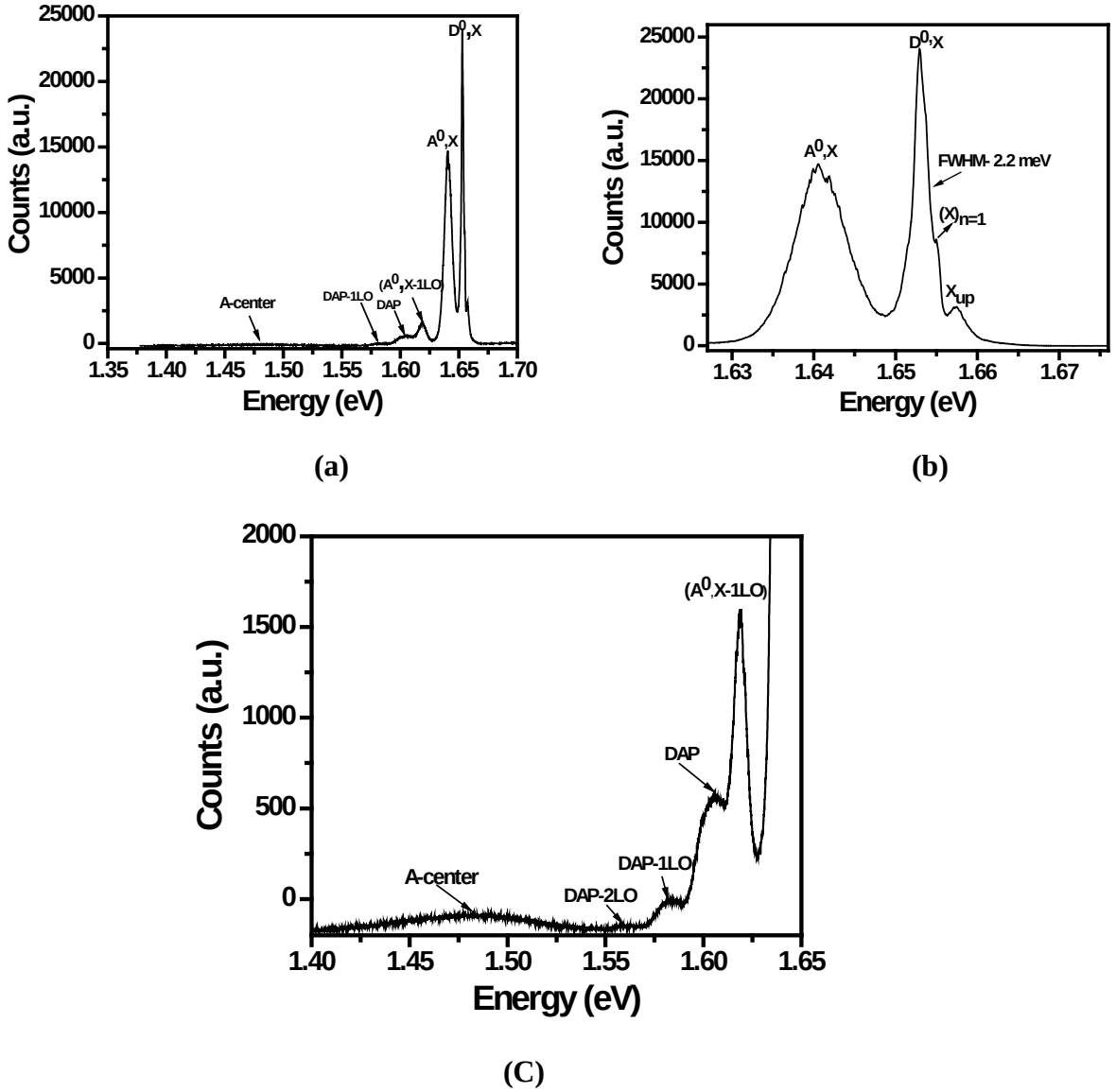

Fig. 6. PL spectra at 5 K of as-grown CZT by THM: a) full spectrum, b) near-band-edge region, and c) donor-acceptor and defect band regions.

The broad band centered at ~ 1.48 eV is the defect band, assigned as A-center; it agrees well with the literature [13, 15]. The A-center peak originates due to the Cd vacancy-In complex.

The charge transport properties of our as-grown CZT samples were investigated up to a thickness of 10 mm. The $(\mu\tau)_e$ values varied from $6x10^{-3}$ to $2x10^{-2}$ cm^2/V for different ingots, with the best mobility of 968±1.5% cm^2/V-sec. The resistivities of the as-grown samples for different ingots were found to be consistently in the range of $1\text{-}3x10^{10}$ ohm-cm. The internal electric fields were found to deviate from the ideal ones; they are comparable to those observed for commercially available CZT samples. Many detectors of different volumes were fabricated from the as-grown ingots. The as-grown samples showed fairly good detector response with resolutions of ~1.5%, 2.7% and 3.8% at 662 keV for a quasi-hemispherical geometry for detector volumes of 0.18 cm^3, 1 cm^3 and 4.2 cm^3, respectively. Here, no electron charge-loss corrections were used; much better energy resolutions are expected once this correction factor is implemented in the analysis.

SUMMARY

In this present study we have investigated the size distribution and concentration of Te inclusions/precipitations for our as-grown CZT samples by a modified THM technique. The study reveals that by controlling the growth interface, it is possible to reduce the concentration and size of the Te inclusions/precipitations, resulting in better as-grown detector quality CZT by THM technique. The reported simulated results suggest that the size distribution and concentration of Te inclusions/precipitations in our as-grown sample are capable of fabricating 15-mm-thick detectors. The PL and excellent charge transport properties also reflects the good quality of our as-grown samples. The observed 3.8% resolution for 16-mm thick detectors with a volume slightly more than 4 cm^3, excellent charge transport properties, and high crystal quality offer promise for fabricating low-cost large-volume working detectors from as-grown ingots (i.e., no post-growth thermal annealing step).

REFERENCES

1. H. Chen, S. A. Awadalla, K. Iniewski, P. H. Lu, F. Harris, J. Mackenzie, T. Hasanen, W. Chen, R. Redden, G. Bindley, Irfan Kuvvetli, Carl Budtz Jørgensen, P. Luke, M. Amman, J. S. Lee, A. E. Bolotnikov, G. S. Camarda, Y. Cui, A. Hossain and R. B. James, J. Appl. Phys. **103**, 014903 (2008).
2. S. A. Awadalla, H. Chen, J. Mackenzie, P. Lu, K. Iniewski, P. Marthandam, R. Redden, G. Bindley, Z. He and F. Zhang, J. Appl. Phys. **105**, 114910 (2009).
3. A. El Mokri, R. Triboulet, A. Lusson, A. Tromnos-Carli and G. Didier, J. Cryst. Growth **138,** 168 (1994).
4. H. Chen, S. A. Awadalla, J. Mackenzie, R. Redden, G. Bindley, A. E. Bolotnikov, G. S. Camarda, G. Carini and R. B. James, IEEE Transactions on Nuclear Science **54,** 811 (2007).
5. R. Schoenholz, R. Dian and R. Nitsche, J. Cryst. Growth **72**, 72 (1985).
6. G. Yang, A.E. Bolotnikov, Y. Cui, G.S. Camarda, A. Hossain and R.B james, J. Cryst. Growth 311 (2008) 99.
7. A.E. Bolotnikov, G.S. Camarda, G.A. Carnini, Y. Cui, L. Li and R.B. James, Nucl. Instr. Meth. Phys. Res. **A 571**, 687 (2007).

8. D. S. Bale, J. Appl. Phys. 107 (2010) 014519.A. E. Bolotnikov, G. S. Camarda, G. A. Carnini, Y. Cui, L. Li and R. B. James, Nucl. Instr. Meth. Phys. Res. **A 571**, 687 (2007).
9. U. N. Roy, A. Gueorguiev, S. Weiler and J. Stein, J. Cryst. Growth **312**, 33 (2010).
10. A. E. Bolotnikov, N. A-Jabbar, O. S. Babalola, G. S. Camarda, Y. Cui, A. Hossain, E. M. Jackson, H. C. Jackson, J. A. James, K. T. Kohman, A. L. Luryi and R. B. James, IEEE Trans. on Nucl. Sci. **55**, 2757 (2008).
11. A. E. Bolotnikov, O. S. Babalola, G. S. Camarda, Y. Cui, S. U. Egarievwe, R. Hawrami, A. Hossain, G. Yang and R. B. James, IEEE Trans. on Nucl. Science **57**, 910 (2010).
12. A. E. Bolotnikov, G. S. Camarda, G. A. Carini, Y. Cui, K. T. Kohman, L. Li, M. B. Salomon and R. B. James, IEEE Trans. on Nucl. Science **54**, 821 (2007).
13. J. E. Toney, B. A. Brunett, T. E. Schlesinger, J. M. Van Scyoc, R. B. James, M. Schieber, M. Goorsky, H. Yoon, E. Eissler, and C. Johnson, Nucl. Instrum. Methods **A 380**, 132 (1996).
14. T. E. Schlesinger, J. E. Toney, H. Yoon, E. Y. Lee, B. A. Brunett, L. Franks and R. B. James, Materials Sc. and Engr. Reports **32,** 103 (2001).
15. G. Yang, W. Jie, Q. Li, T. Wang, G. Li and H. Hua, J. Cryst. Growth **283,** 431 (2005).